

To: Ms. Patricia Poire
Executive Director
Kern Groundwater Authority
1800 30th Street, Suite 280
Bakersfield, CA 93301

Subject: Report Updated Differential Interferometric Synthetic Aperture Radar (DInSAR)
Study of Subsidence in the Kern County Subbasin (KCS)

Earth Consultants International (ECI) are pleased to present this report describing the scope of work, methodology, findings, and conclusions of a Differential Interferometric Synthetic Aperture Radar (DInSAR) study of the KCS. The purpose of this study was to assess the magnitude and potential drivers of land subsidence within the KCS using the latest available Sentinel-1 satellite data.

DInSAR imagery for this study was obtained from Sentinel-1 radar images combined with a Short Baseline Subset (SBAS) stacking algorithm to create (1) a time series to measure subsidence and (2) figures showing the measured average subsidence rates within the KCS for the period January 2019 to December 2021. No Sentinel-1 data was included after December 2021 as an onboard power issue caused the Sentinel-1B spacecraft to malfunction on December 23, 2021. The loss of Sentinel-1B data led to degradation of the resolution of the stacked interferometry of imagery acquired during 2022. For this reason, data from 2022 was not included in this study. To achieve maximum resolution ECI downloaded, processed and analyzed a total of 90 Sentinel-1 SAR images dating from January 3, 2019, to December 19, 2021. This data represents the period spanning from the end of the by ECI previously stacked Sentinel-1 data (with overlap) used in its 2021 report, to the end of December 2021 when Sentinel-1B stopped producing usable data. In total the DInSAR stack generated by ECI contained 342 interferograms spanning the period of interest (i.e., 2019-2021 for this current study). The DInSAR stack was then corrected against the permanent GPS station "ISLK" located near Lake Isabella. It should be noted that due to issues with some SAR images in the frame immediately north of the target area, these data had to be excluded when processing the SAR imagery. Due to this, part of the northern end of AOI-1 and western end of AOI-5 is missing and data from the 2021 interferometric stack has been utilized for this area. This was possible as an analysis of the border area in AOI-5 showed that the subsidence rates are very similar on either side of the edge where data is missing in this study.

For presentation, the processed output of the interferometric stack was converted from millimeters to inches and the cumulative subsidence was classified into 13 color coded intervals ranging from 1 to >40 inches. To the extent possible ECI utilized the same color coding as those provided in previous NASA/JPL figures covering the area.

Figure 1a presents cumulative subsidence as presented in the ECI (2021) report for the period 1/4/2015 to 9/30/2020. The raw cumulative and annual displacement (i.e., subsidence) data was used to create eight time series transects at select locations. **Figures 1b and 2** present the current study period cumulative subsidence and annual rate of subsidence, respectively. For this study as noted above, ECI

was unable to process InSAR data for a wedge-shaped area in the northwestern part of the Basin. This was due to several “broken” SAR images for the frame immediately north of the study area. To maintain the highest resolution possible, and reduce temporal and spatial noise, this area was not included in the data processing. ECI is assessing how to mitigate this issue in order to reduce temporal noise in any future analysis. The locations of the individual time series transects are shown in **Figure 3**.

For calibration of the interferometry the continuously operating GPS station ‘ISLK’ near Lake Isabella was selected as it is near to the study area, and it shows near zero vertical movement over time.

The ECI subsidence maps, point time series and subsidence transects verify the general subsidence patterns identified by earlier investigations by NASA/JPL (Farr et al 2015, 2016), TRE Altamira (2019) and the statistical study of the TRE Altamira report done by Towill, Inc (2020) commissioned by the Department of Water Resources (DWR). In addition, the data comports well to the previous study by Earth Consultants International, Inc (2021).

This current study verifies the results in the previous ECI report, that the subsidence rates are significantly lower (45-50%) than the previous JPL/NASA study of 2020 reported. The subject study also verifies the recent subsidence rates measured by TRE ALTAMIRA on behalf of the DWR. Additionally, the time-series transects indicate that there is a secondary, larger, area of subsidence around the Lost Hills Oil Field (AOI-2), that is driven by non-SGMA-related factors. This finding is contrary to historical reports by others that assumed that agriculture was a principal cause of subsidence in the vicinity of Lost Hills (i.e., Aqueduct mile posts 195 to 215). A similar phenomenon is also evident in AOI-4.

We appreciate the opportunity to provide these services to the KCS. Should you have any questions regarding the above, please do not hesitate to contact us at your earliest convenience.

Respectfully submitted,

EARTH CONSULTANTS INTERNATIONAL, INC.

Registered Geologists, Certified Engineering Geologists and Certified Hydrogeologists

Anders Hogrelius, PG 9693
Senior Project Consultant

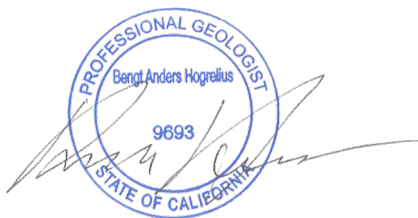


TABLE of CONTENTS

Section	Page No
1.0 INTRODUCTION	1
1.1 PURPOSE OF THE STUDY	1
1.2 FINDINGS OF 2021 STUDY	1
2.0 TECHNICAL BACKGROUND	3
3.0 CURRENT STUDY AND METHODOLOGY.....	4
3.1 INSAR PROCESSING OF SENTINEL-1 DATA, COMBINING AND STACKING INTERFEROGRAMS	4
3.4 CORRELATING DINSAR VELOCITIES WITH GPS CALIBRATED PSEUDO-VERTICAL INTERFEROMETRY DATA	5
3.5 EXTRACTION OF TRANSECTS AND POINT TIME SERIES.....	5
4.0 FINDINGS AND DISCUSSION	6
4.1 SUBSIDENCE WITHIN THE KERN COUNTY SUBBASIN.....	6
5.0 CONCLUSIONS AND RECOMMENDATIONS.....	9
5.1 CONCLUSIONS	9
5.2 RECOMMENDATIONS.....	10
6.0 REFERENCES CITED.....	11

FIGURES

Figure 1a.	Cumulative Subsidence 1/4/2015 to 9/30/2020
Figure 1b.	Cumulative Subsidence 1/15/2019 to 12/18/2021
Figure 2.	Subsidence Rate Map 3/1/2019 to 18/12/2021.
Figure 3.	Locations of Time Series Transects.
Figure 4.	Locations of AOI-1 through AOI-5.
Figure 5a-5h.	Time Series for Tracks A-A' to H-H', AOI's 1 through AOI 5.



**Differential Interferometric Synthetic Aperture Radar (DInSAR)
Study of Subsidence in the Kern County Subbasin (KCS)**



1.0 INTRODUCTION

1.1 PURPOSE OF THE STUDY

Earth Consultants International (ECI) conducted a ground deformation (subsidence) study for the Kern County Subbasin (KCS, subbasin, or Subbasin) area using stacked satellite-based Differential Interferometry Synthetic Aperture Radar (DInSAR). The purpose of the study was to assess and refine the understanding of the magnitude and causes of land subsidence within the KCS with a focus on previously identified areas of interest (AOI) and regional critical infrastructure in the KCS.

1.2 FINDINGS OF 2021 STUDY

The previous (2021) study by ECI/Aquilogic concluded that:

- Sentinel-1 SAR data provides a viable method of mapping and monitoring subsidence within the KCS, especially when combined with a stacking method that reduces atmospheric noise and that allows the data set to be reliably calibrated against continuous GPS stations in the area.
- The vertical resolution of the DInSAR stack for the study is approximately 2.4mm/year (0.09 inch/year) based on comparisons with data from KCS continuous GPS stations in the study area. The error rate is approximately 2.4mm/year (one standard deviation).
- Though subsidence rates identified in the 2021 study require careful future monitoring, we have concluded previous studies by others may be overestimating by 45 to 50% the subsidence rates associated with seasonal groundwater extraction within the KCS. This is due to the short time intervals related to the acquisition of available InSAR data (Confirmed by JPL, Personal communication with Dr. Zhen Liu, 2021).
- The northern boundary of the KCS is administrative and not hydraulically based. Groundwater extraction activities to the north of the KCS have resulted in significant and persistent subsidence. This condition should be considered in SGMA related planning by the KCS, and be included in future monitoring as these extraction activities contribute to the subsidence in areas along the northern KCS boundary.
- Although subsidence is generally envisioned to be primarily vertical phenomenon, there is also a horizontal stress (3-dimensional) geomechanical component to subsidence that can have profound effects on infrastructure such as aqueducts, canals pipelines and well casings.
- Discerning the difference between subsidence caused by seasonal (cyclical) groundwater extraction and non-seasonal (i.e., long term non-SGMA) activities is possible utilizing DInSAR. The ability to ascertain these differences are enhanced when DInSAR is integrated with GPS or location-specific ground-based technology (e.g., extensometers, new GPS stations etc.).



Additionally, the 2021 study found the following for the KCS defined Areas of Interest (AOI's) 1 to 5:

Friant-Kern Canal (AOI 1)

AOI-1 encompasses Friant- Kern Canal Mileposts 120 to 130, east-northeast of the City of McFarland (**Figure 4**). At times, previous InSAR monitoring by others has detected up to 5 inches per year of subsidence in areas surrounding this segment of the Friant-Kern Canal. These rates were likely an over estimation. The ECI 2021 study indicated that the rate of annual subsidence in this AOI averages between 2 and 3 inches/year.

California Aqueduct Mileposts 196 to 215 (AOI 2)

AOI-2 consists of a segment of the Aqueduct between Mileposts 195 to 215 (**Figure 4**). Studies by the Kern Groundwater Authority (KGA) and Westside Districts Water Authority (WDWA) in 2019 and early 2020 identified LOHF activities and geotechnical issues as key contributing factors to the identified subsidence. The ECI 2021 study confirmed that the subsidence along this segment of the Aqueduct displays the characteristics of non-SGMA factors, and that the LHOE is isolated by areas of generally lower annual subsidence, suggesting that agricultural groundwater extraction is minimal in this area. According to historical documents this segment of the Aqueduct was not hydro-compacted prior to construction.

Friant-Kern Canal Mileposts 130 to 137 (AOI 3)

AOI-3 is located along the Friant-Kern Canal between Mileposts 130 and 137, southwest of the town of Famoso and the Poso Creek drainage (**Figure 4**). Annual subsidence rates identified by the 2021 study were estimated to range between 2 to 3 inches/year. The principal cause is agricultural pumping. An area of higher annual rate of subsidence (minimum of 3 inches/year) is located immediately to the west of AOI 3. That subsidence is also attributable to agricultural activities. The Friant Water Authority and the United States Geological Survey (USGS) are installing a new extensometer in AOI-3 in late 2023.

California Aqueduct Mileposts 264 to 271 (AOI 4)

AOI-4 is located between Aqueduct Mileposts 262 and 276 (**Figure 4**). A review of the NASA/JPL rate of subsidence for 2015-2016 indicated that this area experienced between 2 and 4 inches of subsidence for that period. As noted in the 2021 study these rates are likely an overestimate. Data provided in the ECI 2021 study found an average subsidence rate for the period April 2015 to September 2020 to be around 1 to 2 inches/year. Sources are believed to be a combination of factors including geotechnical, oilfield activities, and agricultural pumping.

North Boundary of Subbasin (AOI 5)

AOI-5 is located along the northern boundary of Kern County (**Figure 4**). While there reportedly is no large critical infrastructure within AOI-5, there are many individual well casings that could be affected by localized subsidence. Coordinated monitoring with adjacent GSAs, both within the KCS, and adjacent GSAs outside of the KCS to the north was recommended. A review of the rate of subsidence for 2015-2016 presented in the 2020 NASA/JPL data showed that this AOI reportedly experienced between 5 and 8 inches of subsidence for that period. Data provided in the ECI 2021 study indicated an average subsidence rate for the period April 2015 to September 2020 of around 2 to 4 inches/year, with isolated areas slightly higher. The cumulative subsidence for the ECI 2021 study period was approximately 5 to 10 inches versus 10 to 15 inches for the period 2015 to 2017 as presented in the NASA/JPL data. It appeared that areas immediately to the north of AOI- 5 and outside of the KCS are experiencing significantly higher cumulative subsidence ranging from between 20 to 40 inches in places during the ECI 2021 study period.



2.0 TECHNICAL BACKGROUND

The KCS has been defined as a High Priority subbasin pursuant to the California Sustainable Groundwater Management Act (SGMA). In correspondence dated March 2023 the Department of Water Resources (DWR) determined that the KCS had submitted inadequate Groundwater Sustainability Plans (GSPs) and specifically identified KCS proposed approaches for the coordinated monitoring and addressing of subsidence undesirable results as being deficient. Of special interest to the DWR are potential effects on identified regional critical infrastructure (e.g., California Aqueduct, Friant-Kern Canal) and the five previously identified subsidence AOIs within the KCS.

Historically, it was commonly believed that the principal cause of subsidence in the Subbasin and Central Valley at large was groundwater extraction for agriculture and municipal use. However, recent separate subsidence studies to fill identified data gaps conducted by the WDWA, the KGA have found that the underlying causes of subsidence in the KCS are more complex and likely include several interrelated factors, not all of which are SGMA-related. Among these factors are groundwater extraction for beneficial use, exempt oilfield activities and geotechnical conditions related to the disparate types of soil native to the KCS, age of the Aqueduct, natural settlement due to ongoing geologic sedimentation in the subbasin, and orogeny. The paper *“Pliocene–Quaternary subsidence and exhumation of the southeastern San Joaquin Basin, California, in response to mantle lithosphere removal.”* by M. Robinson Cecil et al, 2014, describes tectonic processes in the mantle that cause deformation under the eastern part of the KCS that can affect deformation. This current study by ECI was designed to further refine the understanding of the causes and magnitude of subsidence in the KCS, and if possible, separate anthropogenic subsidence from subsidence driven by natural and non-SGMA processes.

To assess varying subsidence processes within the sub-basin, which include groundwater pumping for agricultural, industrial, and exempt oil and gas extraction, the subbasin has been sub-divided into Eastern, Western, Southern, and Central Regions. (Figure 4). The boundaries for these areas encompass generally similar hydrogeology and groundwater uses.

The West Region of the KCS is distinguished by extensive areas of open range land and oil field operations interspersed with some cultivated lands. Sediments generally thin westward toward the margins of the subbasin and geologic folding is common. Clays are typically thin, discontinuous or absent in places. Much of the Westside has no significant current or planned groundwater use because of naturally poor water quality due to the presence of marine sediments and saline connate water. As such, domestic wells are scarce in the west. Banked surface water and surface water deliveries from the State Water Project (SWP) via the Aqueduct are a primary source of water for agriculture. Groundwater is primarily used for blending when surface supplies are reduced. Significant volumes of oil field “produced water” are generated in the west region. Produced water is a by-product of oil production common to almost all oil fields in the KCS. Produced water is exempt from SGMA, and therefore outside of the control of the KGA or other GSAs in the KCS. Soils and geotechnical factors are also contributors to subsidence.

The Southern Region is characterized by a mixture of coarse and fine-grained sediments sourced by mountain front alluvial fans. Similar to the Western Region, geologic folding and faulting are present in the Southern Region. Land uses include agriculture and commercial and urban development. SGMA related groundwater extractions include industrial, municipal and agriculture. The Southern Region also



receives surface water delivered by the Aqueduct and other surface water sources. In addition, groundwater is recharged by precipitation and mountain front underflow. Non-SGMA oil field activities are found in proximity to Aqueduct Mile Post 264.

The Eastern Region is roughly bounded on the west by the Friant-Kern Canal and the foothills of the Sierra-Nevada Range on the east. The Region encompasses both municipal, industrial and agricultural use. Non-SGMA oil field activities are also present. Several important aquifers crop out in the foothills and groundwater quality is generally good. Groundwater is utilized for various beneficial uses (e.g., municipal, agriculture, industry). Deliveries of surface water via the Friant-Kern Canal is a primary source of water for agriculture, although not all growers have access to Friant-Kern Canal water.

The Central Region of the KCS is characterized by widespread agricultural activity, interspersed with municipal and industrial uses. Scattered non-SGMA oilfield operations are also present. The Central Region is particularly susceptible to land subsidence caused by groundwater extraction. This is due to the presence of extensive layers of compactible clay (e.g., Corcoran Clay) and other fine-grained sediments in the subsurface. The sources of water for beneficial use include, among others, groundwater, banked surface water, and surface water deliveries from the Aqueduct and Friant-Kern Canal.

It should be noted that not all subsidence in the KCS is inelastic, particularly in zones above the Corcoran Clay and its equivalent clays, or in areas such as the west side and Kern Fan where fine-grained sediments are absent, thin or discontinuous.

3.0 CURRENT STUDY AND METHODOLOGY

To build upon and refine the findings and conclusions of our 2021 Report, The following elements were completed as part of this study. This study evaluates the period 2019 to December 2021.

3.1 INSAR PROCESSING OF SENTINEL-1 DATA, COMBINING AND STACKING INTERFEROGRAMS

A total of 90 Sentinel-1 radar images were downloaded from the European Space Agency (ESA) and processed using the Generic Mapping Tools - Synthetic Aperture Radar (GMTSAR) processor. The 90 SAR images were combined to produce 342 interferograms. By stacking this number of images ECI was able to correct for the effects of ambient moisture in the atmosphere on the interferometric data that often leads to decorrelation. The removal of the atmospheric effects (which can be substantial) due to moisture in clouds, transpiration and fog is important for achieving data accuracy. By using multiple interferograms created from different radar images within the same interferometric dataset, it is possible to calculate, and then subtract, the atmospheric effect on all but the first and last image in the stack. The first and the last slice in the interferometric stack can for that reason contain data outliers.

The second step of the stacking process utilizes a least-squares method on corresponding pixels in every slice of the interferometric stack to extract a map of the surface velocities along LOS from the satellite. In so doing, the potential for data outliers to affect the final result is minimized. The initial stacking and atmospheric corrections are corrected with a Short Baseline Subset (SBAS) algorithm included in the GMTSAR package.



To remove the last traces of atmospheric interference from the interferometric stack, ECI used a calibration process where a stable point (i.e., minimal subsidence) was identified within the footprint of the satellite images and adjacent to the KCS. In this case we used the CORS GPS station ISLK operated by UNAVCO, which shows long-term stability and is located distal to known sources of significant active deformation (i.e., horizontal, subsidence or uplift). All interferograms in the stack were adjusted so the value of the pixels corresponding to the location of the stable reference point are equal to zero (or in general, matching the displacement of the GPS station) and were re-processed with the stacking software to generate maps where the displacement rates are calibrated (i.e., tied to GPS data).

For this study, ECI was unable to process InSAR data for a wedge-shaped area in the northwestern part of the Basin. This was due to several “broken” SAR images for the frame immediately north of the study area. To maintain the highest resolution possible, and reduce temporal and spatial noise, this area was not included in the data processing. ECI is assessing how to mitigate this issue in order to reduce temporal noise in any future analysis.

3.4 CORRELATING DINSAR VELOCITIES WITH GPS CALIBRATED PSEUDO-VERTICAL INTERFEROMETRY DATA

For quality control, stacked, Global Positioning System (GPS) calibrated, vertical velocity data was downloaded from Scripps SAF InSAR Time Series online services (<https://topex.ucsd.edu/gmtsar/insargen/>) for the five AOI’s identified in the KCS (**Figure 4**). The downloaded GPS calibrated data was then compared to the data generated from the interferometric stack.

3.5 EXTRACTION OF TRANSECTS AND POINT TIME SERIES

Pursuant to DWR comments and to further refine the understanding of the causes of subsidence within the five AOI’s and the potential for undesirable effects on identified regional critical infrastructure, we extracted eight transects (**Figures 5a – 5h**). The transects depict annual rates and cumulative displacement between 2019 and 2022. The placement of the transects evaluate identified regional critical infrastructure such as the Aqueduct and the Friant-Kern Canal (**Figure 4**). For orientation purposes, markers showing the location of canals, major roads and oil fields were inserted into the time series transects. Extraction of transects and raster calculations for conversion between millimeters and inches were done with Quantum GIS (QGIS) the resulting text files with the cross sections were subsequently plotted with the Generic Mapping Tools (GMT). A similar technique was used when extracting data from the interferometric stacks. We used GMT to extract the deformation values stored in the pixels at chosen geographic locations in the raster files that makes up the interferometric stack, transferring the values to text files. These files were then plotted in GMT together with data from the continuously operating GPS stations. The time series data was also used to create pseudo-3-D sections (aka wireframe diagram) showing displacement along the transects over time. These graphs were created in Golden Software’s “Surfer” software package by letting the X-axis represent distance along the transect, the Y-axis representing displacement and the Z-axis representing time since the start of the time series.



4.0 FINDINGS AND DISCUSSION

Based on the data reviewed for this report and the ECI 2021 report, we offer the following findings.

4.1 SUBSIDENCE WITHIN THE KERN COUNTY SUBBASIN

The study found that the subsidence rates for the period 2019 – 2021 differ slightly from the findings in the ECI 2021 study. Minimum, maximum and average subsidence rates have been calculated for the KCS **Table 1**. When compared to the 2021 study overall the subsidence rate in the KCS has remained similar or slightly accelerated for some scattered smaller areas (e.g., AOI-4). The likely cause being increased groundwater extraction in combination with the extreme drought conditions in California. In some areas such as AOI-2, AOI-4, and the westside of the subbasin in general, a principal cause of subsidence is non-SGMA activities (i.e., exempt produced water withdrawals). Produced water is formation water that is commingled with oil. Many of the oil fields in Kern County are considered to be “mature” and, as a consequence, have high ratios of produced water to oil. On the west side of the subbasin oilfield extraction occurs in some of the same formations utilized for irrigation (e.g., Tulare formation, etc.). Oil field activities of varying scale are common throughout the KCS.

Due to the malfunction of the Sentinel 1B satellite in December 2021, data from the Sentinel-1 satellite is no longer reliable enough for the generation of detailed SBAS time series and other InSAR data sources may be necessary for future studies. However, DWR and JPL/NASA are continuing to provide data utilizing a permanent scatterer approach for processing.

In addition to subsidence caused by anthropogenic sources (water- and oil/gas extraction), the subsidence patterns in the eastern part of the KCS may be complicated by areas of subsidence and uplift caused by processes in the mantle overprinting the deformation patterns driven by anthropogenic sources (M. Robinson Cecil et al, 2014). As it is impossible to separate the two sources using InSAR alone, it may be necessary to use numerical modeling based on the findings in this paper to separate the two sources of surface deformation.

Based on this study period (2019 to 2021) the range of subsidence in inches per year within the four individual Subbasin Regions are:

	Max Subsidence	Median	Mean	Max Uplift
West Region:	-11.26	-0.71	-1.05	1.95
South Region:	-4.24	-1.12	-1.21	0.23
East Region:	-3.97	-0.79	-0.92	0.04
Central Region:	-12.52	-1.18	-1.45	0.17

Table 1. Calculated basin regional subsidence rates, 2019 to 2021.

These rates are reflective of all basin activities (i.e., SGMA and non-SGMA related).

Based on the various studies conducted by the KGA and KCS to date it is apparent that subsidence is a dynamic condition with many often-interrelated causes, not all of which are SGMA related. Non-SGMA related causes include, but are not limited to geologic processes (e.g., subbasin continuing deposition), geotechnical conditions, soils, age of the infrastructure, and oil field activities. Note that the figures for max subsidence and uplift may be highly localized outliers and are not representative for the subbasin



region as a whole. For example, the maximum subsidence noted in the West region (-11.26 inches/yr.) is associated with activity in the Belridge oil field, and not an identified agricultural area.

The subsidence ranges within the five areas of interest are:

Friant-Kern Canal Mileposts 120 to 130 (AOI-1)

AOI-1 is located along the Friant- Kern Canal between Mileposts 120 to 130, east-northeast of the City of McFarland (**Figure 4**). At times, previous InSAR monitoring has detected up to 5 inches per year of subsidence in areas surrounding this segment of the Friant-Kern Canal. The current study indicates that the rate of annual subsidence in this AOI averages between 1 to 1.6 inches with a marked increase near the border of Tulare County, and that the principal cause of subsidence is groundwater extraction north of the border.

California Aqueduct Mileposts 195 to 215 (AOI-2)

This current study shows the subsidence along this segment of the Aqueduct displays the characteristics of various non-SGMA sources, and that the LHOF is isolated by areas of generally lower annual subsidence, suggesting that subsidence driven by agricultural groundwater extraction is minimal in this area. Subsidence rates ranging between 0.8 and 1.6 inches per year has been detected in this study.

Friant-Kern Canal Mileposts 130 to 137 (AOI-3)

Subsidence rates identified by this current study is estimated at between 0.5 to 2.5 inches and are a result of agricultural activity. An area of higher annual rate of subsidence (minimum of 2.5 inches) is located immediately to the east of AOI 3. Like AOI-1, subsidence is attributable to water extraction due to agricultural activities.

California Aqueduct Mileposts 262 to 276 (AOI-4)

Data in this current study indicates an average subsidence rate for the period January 2019 to December 2021 was around 1 to 3.2 inches. This area includes both SGMA- and non-SGMA-related subsidence such as those associated with geologic structure, coarse-grained alluvial sediments adjacent to the mountain front, and extensive fine-grained surface soils in places due to the former Lake Kern.

North Boundary of Subbasin (AOI-5)

While there is reportedly no regional Critical Infrastructure in AOI-5, there are many individual well casings that could be affected by localized subsidence. Coordinated monitoring with adjacent GSAs, both within the KCS, and those adjacent GSAs outside of the KCS is recommended. A review of the rate of subsidence for 2015-2016 presented in the 2020 NASA/JPL data shows this AOI reportedly experienced between 5 and 8 inches of subsidence for that period. Data provided in this current study indicates a maximum subsidence rate of 8 inches, with an average rate of approximately 1 to 2.5 inches per year, It appears areas immediately to the north of the AOI outside of the KCS are experiencing significantly higher cumulative subsidence related to agricultural activities. (**Figure 4**).

Key findings from the assessment of the DInSAR time series transects are:

- It is possible to discern the difference between a non-SGMA source like oil extraction and seasonal SGMA-related sources like agriculture.



- The time series also show that the effects of oil field activities can extend over a mile from the center of the extraction activity (i.e., crest of the anticline).
- Previous InSAR studies appear to have overestimated the general subsidence rates.
- The results from this study are similar to the subsidence rates detected by Tre Altamira on behalf of the DWR.
- The GPS calibrated Short Baseline Subset (SBAS) method used in this study provides the same or better vertical accuracy as the “Permanent Scatterers” (PSInSAR) method used by DWR/Tre Altamira but with significantly higher spatial resolution. This is due to the fact that the statistical approach used in the SBAS method will include areas with lower correlation but gives them a lower weight when calculating the results, whereas the “Permanent Scatterers” method filters these areas out completely, leaving areas without coverage where the subsidence values have to be interpolated.

A summary of the AOI time series is provided below.

Time Series AOI-1 (Track A-A')

Track A-A' is located between the Eastern and Central Regions and bisects Friant-Kern Canal (**Figure 5a**). The transect displays a wide area of subsidence with a sine wave-like character indicative of agricultural pumping. The Friant-Kern Canal is situated within the band of subsidence at Canal mileposts 120-130.

Time Series AOI-2 (Tracks B-B', C-C', D-D')

These tracks are located in the Western Region and assess subsidence adjacent to the Lost Hills Oil Field and the Aqueduct between Mileposts 195 and 215 (**Figure 5b, 5c, and 5d**). A graph of subsidence along the crest of the oil field (red line) shows a steep slope indicative of robust extraction with significant “noise” due to the vagaries of oil extraction activity. Interestingly, the graphs also show that the effects of the exempt oil extraction extend some distance on either side of the oil field structure visible by the same graph line shapes as those associated with the crest of the oil field. This is important because the Lost Hills Oil Field produces from some of the same formations as those used for irrigation on either side of the oil field (e.g., Tulare and Etchegoin formations).

Time Series AOI-3 (Track E-E')

This time series is also located between the Eastern and Central Regions and is similar to Tack A-A' (AOI-1). AOI-3 includes Friant-Kern Canal Mileposts 130- 137 (**Figure 5e**). The subject time series also displays a signature indicative of agricultural pumping with concomitant subsidence on the Canal. AOI-3 is the location of a planned extensometer to be installed in late 2023 by the Friant Water Authority and the USGS.

Time Series AOI-4 (Track F-F, G-G')

Track F-F' presents a signature indicative of agricultural pumping (blue and green lines on the graph, **Figure 5f**), that appear to have some oil field overprinting (subsidence source contribution) as indicated by the red line on the graph. The oil field influence here is muted, likely because the oil field structure is much smaller than compared to other oil fields like Lost Hills, and there are far fewer oil wells in operation. That said, Aqueduct subsidence in this area is not strictly related to agricultural activity. Track G-G' presents a subsidence signature associated with agricultural pumping. With all three graph lines sharing a similar sine wave type shape. This track is located in the Southern Region near an area of historical subsidence (**Figure 5g**).



Time Series AOI-5 (Track H-H')

This time series is located in AOI-5 along the northern Kern County line (**Figure 5h**). This area is proximal to a prominent subsidence bowl to the north of the KCS located near the towns of Corcoran and Alpaugh. The graph of the times series shows the effects typical of agricultural water extraction. It is important to state that a majority of the drivers behind the subsidence in AOI-5 are located to the north of Kern County. Therefore, the ability to fully mitigate the effects of this subsidence is not within complete control of the Kern Subbasin.

5.0 CONCLUSIONS AND RECOMMENDATIONS

5.1 CONCLUSIONS

Based on the data and methodology presented above, we conclude the following:

- Sentinel-1 SAR data has provided a viable method of mapping subsidence within the KCS when combined stacking and calibration against continuous GPS stations in the area.
- The use of transect time series, showing deformation along a transect over time has proven to be a powerful tool when evaluating the causes driving the subsidence, including discerning the difference between non-SGMA and agricultural causes of subsidence.
- Subsidence generally related to SGMA-related activities is observed in AOIs 1, 3, and 5. Subsidence in AOI-4 appears to be a mixture of SGMA- and non-SGMA-related activities. In AOI-2, subsidence appears to be primarily related to various non-SGMA-related activities.
- The ability to discern the difference between subsidence caused by seasonal (cyclical) groundwater extraction and non-seasonal (e.g., long term non-SGMA) oilfield activities is possible utilizing DInSAR. The ability to ascertain these differences is enhanced when DInSAR is integrated with GPS or location-specific ground-based technology (e.g., extensometers, new GPS stations etc.)
- The average subsidence rates within the KCS has remained similar compared to the end of the previous study by ECI (2021). Only a few scattered areas, including AOI4, is showing increased subsidence compared to the previous study. As groundwater demand reduction is implemented to comply with SGMA, it is possible that the rate of subsidence may attenuate over a longer time frame (i.e., beyond 2040).
- Because of ongoing natural and non-SGMA related activities (e.g., regional subbasin sedimentation, geotechnical factors, soil types, oilfield activities etc.), the rate of subbasin subsidence will never equal “zero”.
- A prominent subsidence bowl immediately north of the Kern County boundary near the towns of Corcoran and Alpaugh are causing undesirable subsidence effects in the subregion.
- AOI-5 and the northern boundary of the KCS is administrative and not hydraulically based. Groundwater extraction activities to the north and within the KCS in this area have contributed



to subsidence rates along this shared boundary. Areas to the north of Kern County are not within control of the KCS.

- Although subsidence is generally envisioned to be primarily vertical phenomenon, there is also a horizontal stress (3-dimensional) geomechanical component to subsidence that can have profound effects on infrastructure such as aqueducts, canals, pipelines and well casings.

5.2 RECOMMENDATIONS

Based on this study, we recommend the following:

1. Conduct additional study to assess whether wet conditions during the winter of 2022-2023 have reduced the subsidence rates in the area along the northern Kern County line (AOI-5) and elsewhere.
2. Three-dimensional forces associated with ground subsidence include horizontal stresses. These stresses can have expensive and long-term undesirable results on critical infrastructure such as the California Aqueduct and the Friant-Kern Canal within the KCS. These forces should be considered and assessed in sustainability management criteria.
3. Continue coordination efforts with GSPs to the north of the KCS with a focus on subsidence monitoring and reporting.
4. Assess whether the combined use of InSAR data and numerical modeling can help differentiate between structurally (orogeny) induced and anthropogenic causes of subsidence on the east side of the subbasin.
5. Assess KCS subsidence on an annual basis and revise/ update time series data a minimum of every five years or as needed based on CASP land survey or other geospatial data.



6.0 REFERENCES CITED

- Amelung, F., Galloway, D.L., Bell, J.W., Zebker, H.A., and Laczniak, R.J., 1999, Sensing the ups and downs of Las Vegas: InSAR reveals structural control of land subsidence and aquifer-system deformation: *Geology*, Vol. 27, pp. 483–486.
- Aquilogic, Inc., 2019, Chapter Groundwater Sustainability Plan Westside District Water Authority Kern County, California
- Aquilogic, Inc., 2020, PowerPoint Presentation, Draft WDWA Subsidence review, presented to the Westside District Water Authority Kern County, California
- Bawden, G.W., 2003, Separating groundwater and hydrocarbon-induced surface deformation from geodetic tectonic contraction measurements across metropolitan Los Angeles, California; *In* Prince, K.R. and Galloway, D.L., (editors), *Proceedings of the Subsidence Interest Group Conference Technical Meeting* held in Galveston, Texas, November 27-29, 2001: U.S. Geological Survey Open-File Report 03-308; available from <http://pubs.usgs.gov/of/2003/ofr03-308/>.
- Borchers, J.W., Carpenter, M., Kretsinger-Grabert, V., Dalgish, B., and Cannon, D., 2014, Land Subsidence from Groundwater Use in California: Water Education Foundation and Luhdorff & Scalmanini Consulting Engineers, 161p.
- California Department of Water Resources (CDWR), 2015, Sustainable Groundwater Management Program Draft Strategic Plan, 31p.
- California Department of Water Resources (CDWR), 2020, SGMA Groundwater Management, <https://water.ca.gov/Programs/Groundwater-Management/SGMA-Groundwater-Management>
- Farr, T., Jones, C.E., Liu, Z., 2017, Jet Propulsion Laboratory, California Institute of Technology, Progress Report: Subsidence in California, March 2015 – September 2016
- Galloway, D.L. and Burbey, T.J., 2011, Review: Regional land subsidence accompanying groundwater extraction: *Hydrogeology Journal*, Vol. 19, No. 8: pp. 1459-1486.
- GEI Consultants, Inc., January 2020, Kern Groundwater Authority Groundwater Sustainability Plan
- Hu, J., Ding, X.L., Lia, Z.W., Zhang, L., Zhu, J.J., Sun, Q., and Gao, G.J., 2016, Vertical and horizontal displacements of Los Angeles from InSAR and GPS time series analysis: Resolving tectonic and anthropogenic motions: *Journal of Geodynamics*, Vol. 99, Sept 2016, pp. 27-38.
- Lanari R., Lundgren P., Mariarosaria M., and Casu, F., 2004, Satellite radar interferometry time-series analysis of surface deformation for Los Angeles, California: *Geophysical Research Letters*, Vol. 31, No. 23, 16 Dec. 2004, 5p.



M. Robinson Cecil, Z. Saleeby, J. Saleeby, K.A. Farley; Pliocene–Quaternary subsidence and exhumation of the southeastern San Joaquin Basin, California, in response to mantle lithosphere removal. *Geosphere* 2014; 10 (1): 129–147. doi: <https://doi.org/10.1130/GES00882.1>

Orange County Water District, 2015, Groundwater Management Plan 2015 Update, 10p.

Poland, J.F., (editor), 1984, Guidebook to Studies of Land Subsidence due to Ground-water Withdrawal: *Studies and Reports in Hydrology*, prepared for the International Hydrological Programme, Working Group 8.4: United Nations Educational, Scientific and Cultural Organization, Paris, France, 305p. plus Appendices; available from <http://unesdoc.unesco.org/images/0006/000651/065167eo.pdf>

Sneed, M., 2016, Land Subsidence: The Lowdown on the Drawdown: US Geological Survey and California Groundwater Resources Association Webinar, March 23, 2016.

Towill, Inc., 2020, InSAR Data Accuracy for California Groundwater Basins, CGPS Data Comparative Analysis January 2015 to September 2019, March 23, 2020.

TRE Altamira, Inc., 2020, InSAR land surveying and mapping services in support of the DWR SGMA program, Technical Report, 16 March 2020.

